DOI: 10.1002/ejic.201600483

Carbene Phosphinidenes

Transition-Metal Carbonyl Complexes and Electron-Donating Properties of N-Heterocyclic-Carbene–Phosphinidene Adducts

Dirk Bockfeld,[a] Adinarayana Doddi,[a] Peter G. Jones,[a] and Matthias Tamm*[a]

Abstract: Rhodium(I), tungsten(0), and molybdenum(0) carbonyl complexes of the N-heterocyclic-carbene–phosphinidene adducts IPr•PR [**1a**, R = H; **1b**, R = Ph; **1c**, R = Mes; IPr = 1,3-bis(2,6-diisopropylphenyl)imidazolin-2-ylidene; Mes = 2,4,6-trimethylphenyl] were prepared. The reaction of **1b** with [Rh(μ-Cl)(CO)$_2$]$_2$ afforded the dicarbonyl rhodium(I) complex *cis*-[(IPr•PPh)RhCl(CO)$_2$] (**2**) as the major product together with the tetranuclear complex [{μ-(IPr•PPh)}$_2$Rh$_4$(μ-Cl)$_4$(CO)$_4$] (**3**). The latter was characterized by X-ray diffraction analysis. The tungsten pentacarbonyl complexes [(IPr•PR)W(CO)$_5$] (**4a**, R = H; **4b**, R = Ph; **4c**, R = Mes) were isolated from the reactions of **1a**–**1c** with [(Me$_3$N)W(CO)$_5$], whereas the reactions of **1a** and **1b** with [(thf)Mo(CO)$_5$] (thf = tetrahydrofuran) gave the corresponding molybdenum complexes [(IPr•PR)Mo(CO)$_5$] (**5a**, R = H; **5b**, R = Ph). The molecular structures of the five carbonyl complexes were established by X-ray diffraction analyses. The IR spectroscopic analysis of the CO stretching frequencies of the carbonyl complexes **2**, **4**, and **5** revealed the strong electron-donating abilities of the phosphorus(I) ligands.

Introduction

In 1997, Arduengo reported the first N-heterocyclic-carbene–phosphinidene adducts (NHC•PR), which were prepared directly through the reactions of free carbenes with cyclic phosphorus(I) compounds such as (PPh)$_5$.[1] Alternatively, an extensive series of similar phenylphosphinidene adducts were synthesized by Bertrand and co-workers through the reactions of stable carbenes with PPhCl$_2$ and subsequent reduction of the resulting phosphorus(III) adducts with 2 equiv. of KC$_8$.[2] These compounds can be represented by structures **A**–**C** (Scheme 1),[3] which reveal their nature as inversely polarized phosphaalkenes.[4,5] As a mesomeric shift towards the polarized form **B** can be expected to afford a more shielded phosphorus atom, the ^{31}P NMR chemical shifts of these adducts were established as an indicator of the π-accepting properties of the respective carbene ligands.[2]

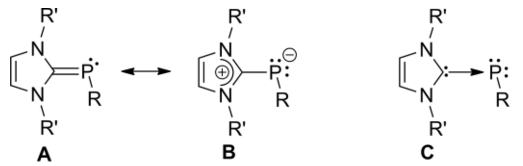

Scheme 1. N-Heterocyclic imidazolin-2-ylidene–phosphinidene adducts; IMes•PPh (R = Ph, R′ = Mes = 2,4,6-trimethylphenyl), IPr•PR (**1a**, R = H; **1b**, R = Ph; **1c**, R = Mes; R′ = Dipp = 2,6-diisopropylphenyl).

Structures **B** and **C** also indicate the possibility that the carbene–phosphinidenes could act as P-donor ligands through two lone pairs of electrons, as was demonstrated by the isolation of the bis(borane) adduct [(IMes•PPh)(BH$_3$)$_2$] [IMes = 1,3-bis(2,4,6-trimethylphenyl)imidazol-2-ylidene] by Arduengo and Cowley.[6] In agreement with the results reported for related phosphinidene systems,[7] this ability was recently confirmed by Dias[8] and our group,[9] who independently prepared a series of coinage metal complexes of the type [(IMes•PPh)(MX)$_2$] and [(IPr•PPh)(MX)$_2$] [IPr = 1,3-bis(2,6-diisopropylphenyl)imidazol-2-ylidene], in which the phosphorus atoms coordinate to two CuCl, AgCl, AuCl, CuBr, or CuOTf (OTf = triflate) moieties. In the latter study, it was also shown that cationic digold complexes such as [(IPr•PPh){Au(tht)}$_2$][SbF$_6$]$_2$ (tht = tetrahydrothiophene) may serve as robust single-source catalysts in cycloisomerization or carbene-transfer reactions, and these were the first applications of carbene–phosphinidenes as ancillary ligands in homogeneous catalysis. Moreover, the isolation of the monometallic complexes [(IPr•PPh)MCl] (M = Cu, Ag, Au) indicates that the stepwise complexation of the phosphorus atom in IPr•PPh is possible.[9] This ability was also demonstrated previously by Lavoie, who reported the ruthenium(II) benzylidene complex [{IMes•PPh}RuCl$_2$(CHPh)(PPh$_3$)].[10]

Adducts of the parent phosphinidene, in particular IPr•PH, have recently attracted much interest, and this species was first generated by Driess and co-workers through silylene-to-carbene PH transfer.[11] Preparative routes were established by Grützmacher from the imidazolium salt (IPrH)Cl by use of Na(OCP) or P$_7$(TMS)$_3$ (TMS = trimethylsilyl) as phosphorus-transfer reagents.[12] Together with Gudat, the same group recently showed that NHC•PH species can also be accessed directly from imidazolium salts and P$_4$ or Na$_3$P$_7$.[13] Na(OCP) also served as the phosphorus source for the synthesis of the more bulky de-

---

[a] *Institut für Anorganische und Analytische Chemie, Technische Universität Braunschweig,*
Hagenring 30, 38106 Braunschweig, Germany
E-mail: m.tamm@tu-bs.de
http://www.tu-braunschweig.de/iaac

Supporting information for this article is available on the WWW under http://dx.doi.org/10.1002/ejic.201600483.

rivative IPr*•PH with 2,6-dibenzhydryl-4-methylphenyl substituents, which was employed by Bertrand to isolate the parent phosphenium species $(IPr^{*}{\bullet}PH_2)^+$ together with the complexes $[(IPr^{*}{\bullet}PH)(BH_3)_2]$, $[(IPr^{*}{\bullet}PH)(AuCl)_2]$, and $[(IPr^{*}{\bullet}PH)Fe(CO)_4]$.[14]

As shown by our group, IPr•PH can also be prepared conveniently from the 2,2-difluoroimidazoline $IPrF_2$ (PhenoFluor™) by reaction with $P(SiMe_3)_3$, followed by desilylation. Notably, the intermediate $IPr{\bullet}PSiMe_3$ was used as a starting material for the synthesis of carbene–phosphinidyne complexes of the type $[(IPr{\bullet}P)ML_n]$ with ML_n = $[(\eta^6\text{-cymene})RuCl]$ or $[(\eta^5\text{-}C_5Me_5)RhCl]$.[15] Related transition-metal complexes such as $[(\eta^5\text{-}C_5Me_5)Fe(CO)_2\{PC(NMe_2)_2\}]$ were reported by Weber,[5,16] and, more recently, Grützmacher described the synthesis of the mercury(II) complex $[Hg(P{\bullet}IMesH_2)_2]$ from the parent phosphinidene adduct $IMesH_2{\bullet}PH$; the latter was prepared from $IMesH_2$ by carbene insertion into the P–H bond of PH_3, followed by dehydrogenation with *ortho*-quinone.[17]

As indicated above, carbene–phosphinidene adducts can be regarded as promising ancillary phosphorus ligands in homogeneous catalysis;[9] therefore, an assessment of their electronic and steric properties is required. Transition-metal carbonyl complexes can be used to study ligand donor properties through the monitoring of their CO stretching frequencies by IR spectroscopy. Arguably, the largest data set is available for rhodium(I) dicarbonyl complexes of the type *cis*-$[(L)RhCl(CO)_2]$[18–20] and, consequently, we describe herein the preparation and characterization of *cis*-$[(IPr{\bullet}PPh)RhCl(CO)_2]$. In addition, a series of tungsten and molybdenum pentacarbonyl complexes of the type $[(IPr{\bullet}PR)M(CO)_5]$ (R = H, Ph, Mes) are reported, and their CO stretching frequencies are compared with those of related phosphine and carbene complexes.[21] It should be noted that these complexes can be regarded as carbene adducts of elusive phosphinidene group VI complexes of the type $[(RP)M(CO)_5]$. According to Mathey, these species can be generated thermally from 7-phosphanorbornadiene complexes, a process that is accompanied by benzene formation, and trapped in situ through (cyclo)addition reactions or the addition of nucleophiles,[22] including a carbene of the diaminocyclopropenylidene-type.[23] A related route was reported recently by Streubel et al. for the preparation of $[\{IMe{\bullet}PR\}W(CO)_5]$ [R = $CH(SiMe_3)_2$, IMe = 1,3,4,5-tetramethylimidazol-2-ylidene], which proceeds through the formation of an anionic phosphinidenoid complex $[(RPCl)W(CO)_5]^-$.[24]

Results and Discussion

Reaction of IPr•PPh with $[Rh(\mu\text{-}Cl)(CO)_2]_2$

The carbene–phosphinidene adduct IPr•PPh (**1b**), prepared by the Bertrand route,[2] was treated with 0.5 equiv. of $[Rh(\mu\text{-}Cl)(CO)_2]_2$ in toluene at room temperature to afford a dark red solution and small amounts of an orange precipitate. The solution was filtered, the solvent was evaporated, and the solid was washed with hexane to furnish the desired complex *cis*-$[(IPr{\bullet}PPh)RhCl(CO)_2]$ (**2**) in analytically pure form in 62 % yield, as indicated by elemental analysis and NMR spectroscopy (see below). The recrystallization of the remaining orange solid gave single crystals suitable for X-ray diffraction analysis, which confirmed the connectivity and formation of the tetrametallic complex **3** (Scheme 2; see Supporting Information, Figure S1 for an ORTEP representation). The formation of the minor product **3** shows that **1b** and related carbene–phosphinidene species are able to bridge two metal atoms; this is accompanied by loss of two CO ligands and dimerization to form $[\{\mu_2\text{-}(IPr{\bullet}PPh)\}_2Rh_4(\mu\text{-}Cl)_4(CO)_4]$, in which the four rhodium atoms are connected by two different types of bridging chlorine atoms.

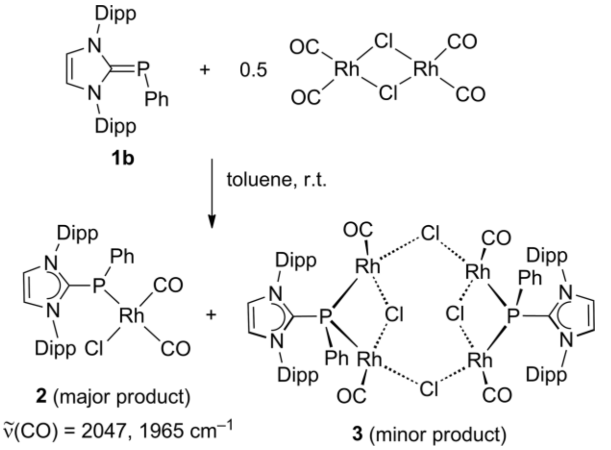

Scheme 2. Synthesis of the carbene–phosphinidene rhodium(I) complexes **2** and **3**.

The presence of two carbonyl groups in **2** is confirmed by its ^{13}C NMR spectrum, which shows two doublets of doublets at δ = 184.7 ($^1J_{Rh,C}$ = 72.0, $^2J_{P,C}$ = 22.5 Hz) and 183.5 ppm (with almost identical, unassignable $^1J_{Rh,C}$ and $^2J_{P,C}$ coupling constants of 65.7 and 60.9 Hz) that can be assigned to the *cis*- and *trans*-CO ligands, respectively (Figure 1).[25] The signal of the phosphorus-bound carbene carbon atom appears as a doublet at δ = 169.3 ppm ($^1J_{P,C}$ = 98.2 Hz), which is slightly upfield and associated with a somewhat larger coupling constant in comparison with the signal of the free carbene–phosphinidene **1b** (cf. δ = 172.9 ppm, $^1J_{P,C}$ = 83 Hz; all spectra were measured in C_6D_6).[2] Likewise, the ^{31}P NMR signal of **2** is shifted by ca. 10 ppm to higher field and appears as a doublet at δ = –28.9 ppm ($^1J_{Rh,P}$ = 48.4 Hz).

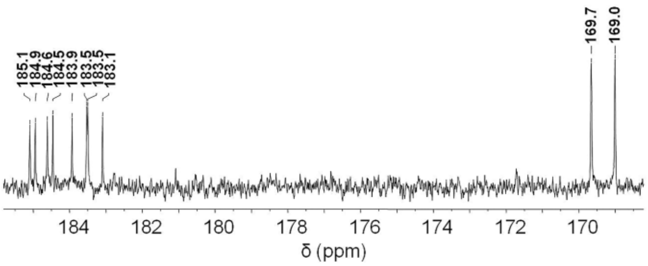

Figure 1. Part of the $^{13}C\{^1H\}$ NMR spectrum of **2** in C_6D_6 at 30 °C.

As expected, the IR spectrum of **2** shows two strong absorptions at $\tilde{\nu}$ = 2047 and 1965 cm^{-1}, which can be assigned to the symmetric and antisymmetric CO stretching vibrations, respectively. From the average value $\tilde{\nu}(CO)_{av}$ = 2006 cm^{-1}, a Tolman electronic parameter (TEP) of 2024 cm^{-1} can be calculated,

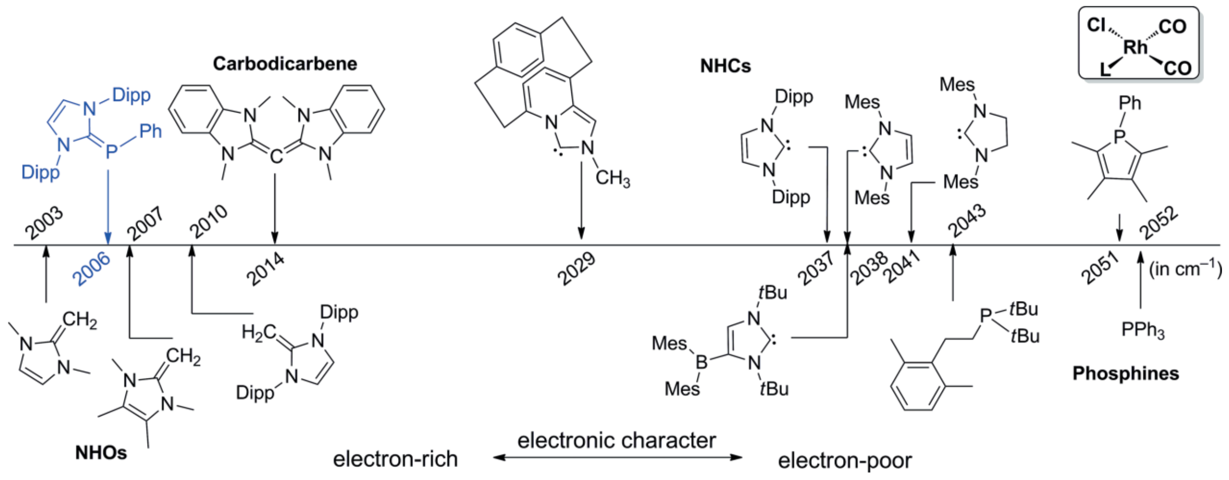

Figure 2. Rhodium scale showing the average carbonyl stretching [$\tilde{\nu}(CO)_{av}$] frequencies of some selected rhodium complexes of the type *cis*-[(L)RhCl(CO)$_2$] (L = carbene, phosphine, etc.).[27,29–37]

which refers to the frequency of the A$_1$ carbonyl mode of complexes of the type [(L)Ni(CO)$_3$].[26] In comparison with the values reported for other phosphorus and carbon donor ligands (Table 1), the low $\tilde{\nu}(CO)_{av}$ and TEP values of **2** indicate very strong Rh–CO π-backbonding and, therefore, a strong electron-donating ability of the IPr•PPh ligand (**1b**). In addition, the relative donor capacities of selected ligands are illustrated in Figure 2, in which the $\tilde{\nu}(CO)_{av}$ values of the respective *cis*-[(L)RhCl(CO)$_2$] complexes are ranked ("rhodium scale").[27]

Table 1. Average CO stretching frequencies and TEPs of a few selected ligands in complexes of the type [(L)Rh(CO)$_2$Cl][a] and [(L)Ni(CO)$_3$].

Ligand	M	$\tilde{\nu}(CO)_{av}$ [cm^{-1}]	TEP [cm^{-1}]	Solvent/method
PPhCl$_2$[28]	Ni	2054	2092	CH$_2$Cl$_2$
P(OPh)$_3$[28]	Ni	2049	2085	CH$_2$Cl$_2$
PPh$_3$[28]	Ni	2029	2068	CH$_2$Cl$_2$
PPh$_3$[29]	Rh	2052	2062	CH$_2$Cl$_2$
PMe$_3$[28]	Ni	2023	2064	CH$_2$Cl$_2$
PCy$_3$[28]	Ni	2015	2056	CH$_2$Cl$_2$
PtBu$_3$[28]	Ni	2014	2056	CH$_2$Cl$_2$
IMes[30]	Rh	2038	2050	CH$_2$Cl$_2$
IPr[29]	Rh	2037	2050	CH$_2$Cl$_2$
Carbodicarbene[31]	Rh	2014	2031	CH$_2$Cl$_2$
IPrCH$_2$[32]	Rh	2010	2029	Nujol
IMe$_4$CH$_2$[33][b]	Rh	2007	2025	ATR[c]
IPr•PPh (**1b**)	Rh	2006	2024	ATR[c]
IMe$_2$CH$_2$[27][d]	Rh	2003	2022	ATR[c]
IMe$_4$CHPh[33][b]	Rh	2002	2022	ATR[c]

[a] TEP = 0.8001$\tilde{\nu}(CO)_{av}$ + 420.0 cm^{-1}.[20] [b] IMe$_4$ = 1,3,4,5-tetramethylimidazol-2-ylidene. [c] Attenuated total reflection. [d] IMe$_2$ = 1,3-dimethylimidazol-2-ylidene.

Accordingly, phosphines and related phosphorus ligands such as phospholes[34] can be regarded as significantly weaker donors than the carbene–phosphinidene **1b**.[29,35] N-Heterocyclic carbenes usually act as stronger donors than phosphines; however, the corresponding $\tilde{\nu}(CO)_{av}$ values,[29,30,36] including those of unusual and rather exotic NHCs,[18,37] are still markedly higher than that of **1b** (Figure 2). A much lower $\tilde{\nu}(CO)_{av}$ of 2014 cm^{-1} was reported for a "carbodicarbene", which displays a similar arrangement of electrons to that of **1b** with two potentially available lone pairs of electrons on the donor atom. A similar polarization of the exocyclic C–C double bond can be accorded to so-called N-heterocyclic olefins (NHOs), which act as similarly strong electron donor ligands in comparison with **1b**.[27,32,33]

Preparation and Characterization of [(IPr•PR)M(CO)$_5$]

Group 6 pentacarbonyl complexes have also been used widely to assess ligand donor properties;[21] therefore, we aimed to prepare the tungsten and molybdenum complexes [(IPr•PR)M(CO)$_5$] (R = H, Ph, Mes; M = Mo, W) by employing the previously reported carbene–phosphinidene adducts **1a** (R = H)[15] and **1b** (R = Ph).[2] In addition, the sterically more encumbered derivative **1c** was synthesized analogously to **1b** through the potassium graphite reduction of the adduct IPr•PMesCl$_2$ obtained from the carbene IPr and dichloromesitylphosphine (PMesCl$_2$). However, **1c** was isolated in only 8 % yield as a yellow solid, whereas Layfield and co-workers recently reported the synthesis of **1c** from [(IPr)Fe{N(SiMe$_3$)$_2$}] and MesPH$_2$ in 57 % yield.[38] In agreement with the reported spectroscopic data, the ^{1}H NMR spectrum of **1c** in C$_6$D$_6$ shows a septet at δ = 3.28 ppm, and two broad signals at δ = 1.45 and 1.08 ppm for the isopropyl CH and CH$_3$ hydrogen atoms indicate hindered rotation around the C$_{carbene}$–P bond. The ^{31}P NMR signal of **1c** in C$_6$D$_6$ is found at δ = –51.3 ppm, which is intermediate between the chemical shifts for **1a** (δ = –133.9 ppm) and **1b** (δ = –18.9 ppm).[2]

Initial attempts to isolate the tungsten pentacarbonyl complex [(IPr•PPh)W(CO)$_5$] (**4b**) involved the photolytically prepared tetrahydrofuran (THF) adduct [(thf)W(CO)$_5$]. The addition of **1b** afforded **4b** in high purity as a precipitate after several days at room temperature but with low and irreproducible yields (ca. 12–34 %). The monitoring of the reaction by ^{31}P NMR spectroscopy revealed that this reaction proceeded slowly even at elevated temperature and with the formation of unidentified side products. The trimethylamine complex [(Me$_3$N)W(CO)$_5$] proved to be a better starting material[39] and afforded **4b** as a yellow crystalline solid in 58 % yield from the reaction with **1b** in THF at 50 °C. Similarly, **4a** was obtained in 57 % yield from **1a**, whereas bulky **1c** gave **4c** in only 18 % yield. The corresponding molybdenum complexes were prepared from thermally generated $[(thf)Mo(CO)_5]$,[39,40] which provided **5a** and **5b** as yellow and pale green solids in 67 and 60 % yield, respectively (Scheme 3). Complexes **4a** and **5a** were isolated as THF solvates, as was also confirmed by X-ray diffraction analysis (vide infra).

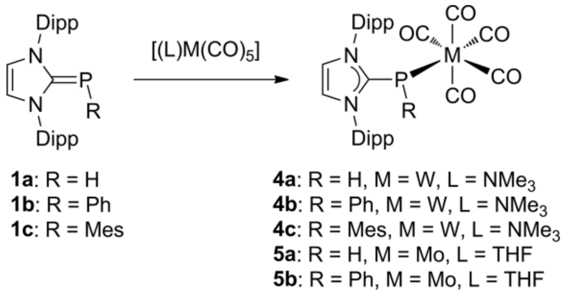

Scheme 3. Synthesis of the carbene–phosphinidene tungsten(0) and molybdenum(0) complexes **4** and **5**.

The pertinent spectroscopic data of **4** and **5** are summarized in Table 2. Unfortunately, the low solubility of the complexes precluded the observation of the ^{13}C NMR signals of the *trans*-CO ligands and, in some cases, the $C_{carbene}$ atoms. For **4a** and **5a**, which contain the parent carbene–phosphinidene IPr·PH (**1a**), the proton-coupled ^{31}P NMR spectra exhibit sharp doublets at δ = –163.4 ($^1J_{P,H}$ = 215 Hz) and –147.1 ppm ($^1J_{P,H}$ = 211 Hz), which are shifted to higher field with an increased P–H coupling in comparison with the signals for **1a**. This resembles the observation reported for the iron tetracarbonyl complex $[(IPr^*{\cdot}PH)Fe(CO)_4]$ (vide supra, δ = –96.4 ppm, $^1J_{P,H}$ = 208 Hz).[14] Similarly, shifts to higher field are also observed for the ^{31}P NMR resonances of **4b**, **4c**, and **5b** upon the metal coordination of **1b** and **1c**, as was also reported for related $W(CO)_5$ complexes of inversely polarized phosphaalkenes such as $[\{tBuP{=}C(NMe_2)_2\}W(CO)_5]$ (δ = –25.1, $^1J_{P,W}$ = 154 Hz).[41] Strikingly, the opposite trend is usually found for phosphine complexes of the type $[(R_3P)W(CO)_5]$, which exhibit shifts of ca. 26 ppm to lower field in comparison with the free PR_3 ligands.[42] These results indicate that metal complexation of the carbene–phosphinidene species **1** leads to a stronger polarization of the carbon–phosphorus double bond, as illustrated by the canonical form **B** (Scheme 1). In addition, a significant spreading of electron density over the $W(CO)_5$ moiety can be proposed on the basis of theoretical calculations.[24] Notably, the coupling constants $^1J(^{31}P,^{183}W)$ of complexes **4** are smaller than those established for $[(R_3P)W(CO)_5]$ complexes (e.g., $^1J_{P,W}$ = 244 Hz for R = Ph)[42] and increase in the order **4a** < **4b** < **4c** (Table 2).

Single crystals of **4a**·THF, **4b**, **4c**, **5a**·THF, and **5b** suitable for X-ray diffraction analysis were grown by cooling saturated solutions in THF to –30 °C. Even though the steric demand of the parent phosphinidene is far lower than that of the phenylphosphinidene moiety, complexes **4a**·THF, **4b**, **5a**·THF, and **5b** crystallize isotypically in the orthorhombic space group *Pbca*. In **4a**·THF and **5a**·THF, the solvent molecules occupy, to a good approximation, the space that is occupied by the phenyl moieties in **4b** and **5b**. The molecular structures of the tungsten complexes **4a** and **4b** are shown in Figures 3 and 4, whereas the molybdenum complexes **5a** and **5b** are presented in the Supporting Information. Complex **4c** crystallizes in the monoclinic space group $P2_1/n$, and the resulting molecular structure is shown in Figure 5. The unit-cell parameters and selected bond lengths and angles are listed in Table 3. In all cases, the formation of pentacarbonyl complexes is confirmed, and they display slightly distorted octahedral geometries around the metal atoms. Similarly to those of other monometallic carbene–phosphinidene complexes,[9,10,24] the phosphorus atoms reside in rather acute trigonal-pyramidal environments, as indicated by angle sums of 329.4, 341.8, and 330.0° in **4b**, **4c**, and **5b**, respectively. The P–M–C4 angles involving the axial carbonyl group are close to linearity for the parent phosphinidene complexes **4a** and **5a** [175.53(17) and 175.63(9)°, respectively], whereas a stronger deviation is observed for the sterically more

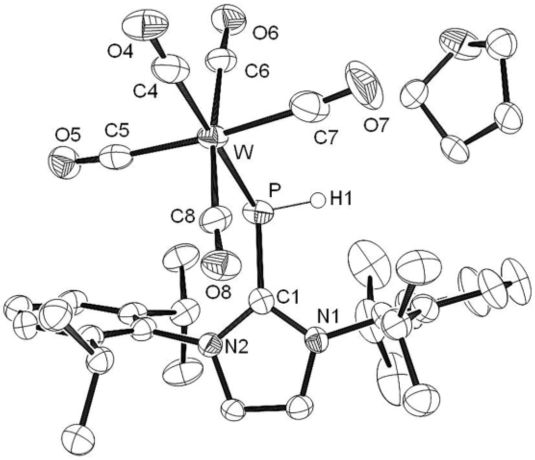

Figure 3. ORTEP diagram of **4a** in **4a**·THF with thermal displacement parameters drawn at the 50 % probability level. Hydrogen atoms are omitted for clarity (except H1); pertinent structural data can be found in Table 3.

Table 2. NMR spectroscopic data of **4** and **5** (L = carbene–phosphinidene).

Complex	δ [ppm] (*J*, Hz)			
	^{31}P		^{13}C of $[(L)M(CO)_5]$ (in $[D_8]THF$)	
	L (in C_6D_6)	$[(L)M(CO)_5]$ (in $[D_8]THF$)	$C_{carbene}$	C_{CO}
4a	–133.9 ($^1J_{P,H}$ = 165)	–163.4 ($^1J_{P,H}$ = 215, $^1J_{P,W}$ = 97)	174.4	199.8
4b	–18.9	–57.7 ($^1J_{P,W}$ = 120)	–	200.9
4c	–51.3	–95.1 ($^1J_{P,W}$ = 159)	–	201.6
5a	–133.9 ($^1J_{P,H}$ = 165)	–147.1 ($^1J_{P,H}$ = 211)	176.2 ($^1J_{C,P}$ = 83)	208.7
5b	–18.9	–40.2	–	–

congested complexes [170.24(10)° in **4b**, 163.39(6)° in **4c**, and 170.45(4)° in **5b**].

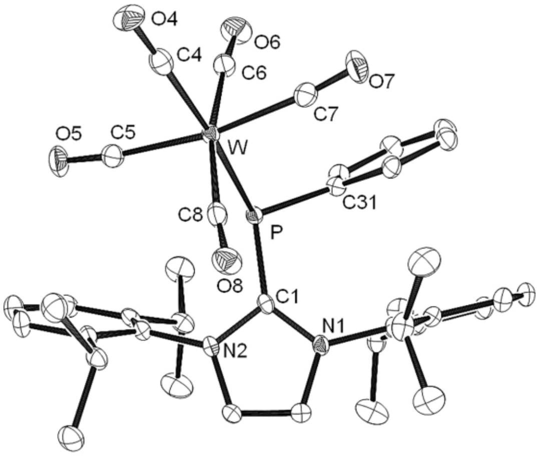

Figure 4. ORTEP diagram of **4b** with thermal displacement parameters drawn at the 50 % probability level. Hydrogen atoms are omitted for clarity; pertinent structural data can be found in Table 3.

The $C_{carbene}$–P bond lengths range from 1.805(2) Å (in **4c**) to 1.819(3) Å (in **4b**) and are significantly longer than those in the free ligands [1.7510(16) Å for R = H,[12] 1.7658(10) Å for R = Ph,[9] 1.766(2) Å for R = Mes],[38] in agreement with the expected decrease of the $C_{carbene}$–P bond order upon metal complexation.[9] The metal–phosphorus bond lengths in the pairs **4a**/**4b** and **5a**/**5b** are almost identical, whereas the steric demand of the mesityl substituent in **4c** affords a slightly elongated W–P bond (Table 3). In comparison, phosphine–pentacarbonyl tungsten and molybdenum complexes such as [(Ph$_3$P)W(CO)$_5$] [2.545(1) Å][43] and [(Ph$_3$P)Mo(CO)$_5$] [2.560(1) Å][44] exhibit markedly shorter M–P distances. In all complexes, the metal–carbon bond to the axial *trans*-CO group is shorter than those to the equatorial *cis*-CO groups, as expected in the presence of a strong σ-donor/weak π-acceptor ligand. This is also reflected by shorter axial M–C4 bonds in comparison with those in [(Ph$_3$P)W(CO)$_5$] [2.006(5) Å][43] and [(Ph$_3$P)Mo(CO)$_5$] [1.995(3) Å].[44]

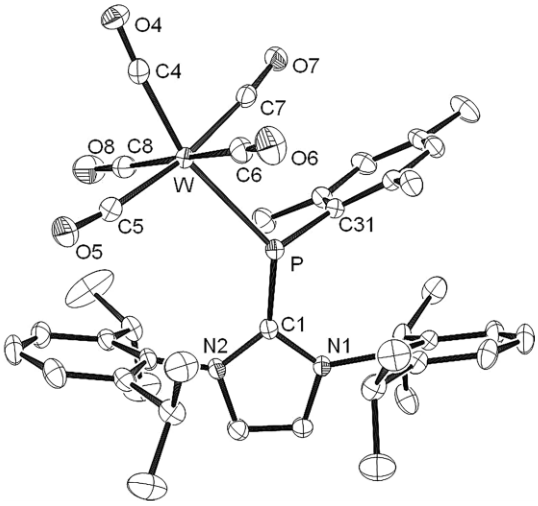

Figure 5. ORTEP diagram of **4c** with thermal displacement parameters drawn at the 50 % probability level. Hydrogen atoms are omitted for clarity; pertinent structural data can be found in Table 3.

In all complexes, the oxygen atom (O5) of one carbonyl ligand points intramolecularly towards one of the 2,6-diisopropylphenyl (Dipp) aryl groups; the resulting distances between O5 and the centroid of the arene ring range from 3.335 (in **4b**) to 3.704 Å (**4c**), which could be cautiously interpreted as weak M–CO(lone pair)•••π(arene) interactions.[45] Some short intermolecular contacts of the type C–H•••O, which indicate weak hydrogen bonds, are observed in the isotypic complexes **4a**, **4b**, **5a**, and **5b**. Short contacts between the hydrogen atoms H3 of the NHC backbone and the axial CO oxygen atoms O4 form chains of molecules parallel to the *b* axis, which are further connected by contacts between the methyl hydrogen atoms of the Dipp moiety and equatorial CO groups (C222–H•••O6) to form planes perpendicular to the *c* axis (see Table 4). The structures of **4a** and **5a** feature additional contacts involving the THF molecule; however, as the THF molecules are disordered in both structures, such contacts should be interpreted with caution. In **4c**, chains parallel to the *a* axis are formed by contacts between

Table 3. Cell parameters and selected bond lengths of **4**–**5**.

	4a·THF	**4b**	**4c**	**5a**·THF	**5b**
Space group	*Pbca*	*Pbca*	$P2_1/n$	*Pbca*	*Pbca*
a [Å]	14.5504(4)	14.9384(6)	10.13568(10)	14.5765(4)	14.95011(10)
b [Å]	18.9292(4)	18.0388(6)	19.0478(2)	18.9211(3)	18.05522(16)
c [Å]	26.5711(9)	26.1322(8)	20.1863(2)	26.5983(6)	26.1307(2)
β [°]	90	90	99.2915(8)	90	90
P–C1 [Å]	1.818(5)	1.819(3)	1.805(2)	1.808(3)	1.8165(14)
P–C31 [Å]	–	1.847(3)	1.851(2)	–	1.8408(14)
M–P [Å]	2.6030(13)	2.6067(7)	2.6224(5)	2.6249(7)	2.6158(4)
M–C4(ax.) [Å]	1.985(6)	1.984(3)	1.976(2)	1.984(3)	1.9790(15)
M–C(eq.)$_{av}$ [Å]	2.049(6)	2.051(4)	2.049(2)	2.045(3)	2.0509(16)
C1–P–C31 [°]	–	105.42(14)	101.65(9)	–	105.65(6)
C1–P–M [°]	114.73(15)	115.22(9)	133.50(6)	115.25(8)	115.47(4)
C31–P–M [°]	–	108.75(10)	106.69(7)	–	108.91(5)
M–P–C4 [°]	175.53(17)	170.24(10)	163.39(6)	175.63(9)	170.45(4)
N1–C1–N2 [°]	104.8(4)	104.7(3)	104.30(16)	105.4(2)	104.92(11)
N1–C1–P–C31 [°]	–	10.7(3)	52.36(18)	–	10.93(15)
N2–C1–P–M [°]	82.0(4)	76.8(2)	16.6(2)	80.7(2)	76.52(11)

the NHC backbones and axial CO groups [C3–H3 0.95 Å, H3•••O7 2.55 Å, C3•••O7 3.380(3) Å, C3–H3•••O7 146.0°; the hydrogen atoms were not refined freely].

Table 4. Short contacts in **4a**, **4b**, **5a**, and **5b** (the hydrogen atoms were not refined freely).

	4a	**4b**	**5a**	**5b**
C3–H3 [Å]	0.95	0.95	0.95	0.95
H3•••O4 [Å]	2.49	2.45	2.50	2.45
C3•••O4 [Å]	3.323(6)	3.237(4)	3.339(3)	3.2376(18)
O4•••H3–C3 [°]	145.9	140.5	146.5	140.4
C222–H [Å]	0.98	0.98	0.98	0.98
H•••O6 [Å]	2.54	2.59	2.55	2.61
C222•••O6 [Å]	3.522(7)	3.526(5)	3.522(4)	3.534(2)
C222–H•••O6 [°]	175.3	158.8	171.7	157.6

The IR spectra of **4a**–**4c**, **5a**, and **5b** exhibit four carbonyl stretching bands. For [(L)M(CO)$_5$] complexes with idealized C_{4v} symmetry, three IR-active CO stretching modes are expected: an $A_1^{(1)}$ vibration, which can essentially be assigned to the stretching of the axial carbonyl group, and two additional vibrations of $A_1^{(2)}$ and E symmetry, which represent the stretching of the equatorial carbonyl groups. If the symmetry of the complexes is lowered by the ligand L, as in the C_1-symmetric complexes **4** and **5**, a fourth band of weak intensity is usually observed and corresponds to the B_1 fundamental.[46] As an example, the IR spectrum of the tungsten complex **4b** is shown in Figure 6.

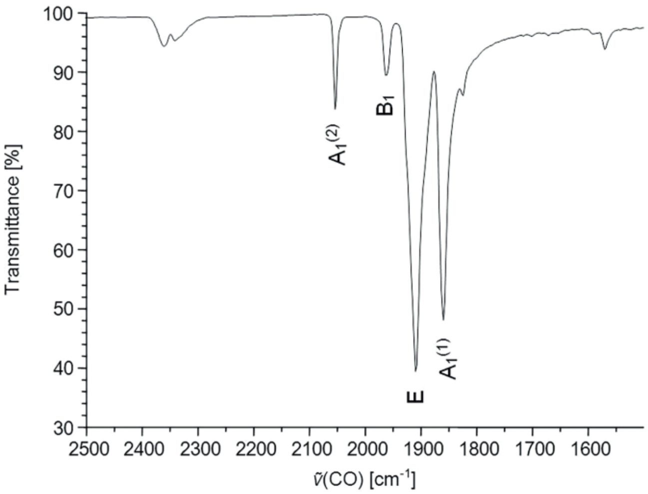

Figure 6. Excerpt from the infrared spectrum of **4b**.

The IR CO stretching frequencies of **4** and **5** together with those of representative phosphine, NHC, and phosphaalkene pentacarbonyl tungsten and molybdenum complexes are summarized in Table 5. In agreement with the results obtained for the rhodium(I) complex **2** (vide supra), the stronger electron-donating properties of the carbene–phosphinidenes **1a**–**1c** in comparison with those of phosphine and NHC ligands is confirmed by the observation of consistently lower CO stretching frequencies. Furthermore, these values agree well with those reported for complexes containing related polarized phosphaalkenes, for example, [{*t*BuP=C(NMe$_2$)$_2$}W(CO)$_5$].[41] Finally, it should be noted that the CO stretching frequencies of **4a** and **4b** as well as those of **5a** and **5b** are very similar; therefore, **1a** and **1b** have similar donor properties, whereas the higher values for **4c** indicate a slightly reduced donating ability of the mesityl derivative **1c**. The latter observation could tentatively be ascribed to a less favorable phosphorus–metal interaction because of steric overcrowding.

Table 5. CO stretching frequencies of various [LM(CO)$_5$] complexes.

L	M	$A_1^{(2)}$ [cm^{-1}]	B_1 [cm^{-1}]	E [cm^{-1}]	$A_1^{(1)}$ [cm^{-1}]	Solvent/method
P(OPh)$_3$[47]	W	2083	–	1958	1965	cyclohexane
PPh$_3$[48]	W	2072	–	1942	1939	cyclohexane
PMe$_3$[48]	W	2070	–	1947	1937	cyclohexane
P*t*Bu$_3$[49]	W	2068	1970	1934	1929	*n*-pentane
IPr[50]	W	2056	1981	1918	1880	Nujol
1c	W	2058	1964	1912	1869	ATR
*t*BuPC(NMe$_2$)$_2$[41]	W	2054	–	1909	1868	KBr
1a	W	2055	1961	1902	1861	ATR
1b	W	2054	1963	1909	1860	ATR
PPh$_3$[51]	Mo	2073	–	–	1946	CH$_2$Cl$_2$
P*t*Bu$_3$[49]	Mo	2069	1978	1935	1936	*n*-pentane
IPr	Mo	2057	–	1921	1882	ATR[a]
1a	Mo	2057	1970	1910	1866	ATR
1b	Mo	2055	1970	1915	1864	ATR

[a] [(IPr)Mo(CO)$_5$] was prepared by the procedure reported for (IPr)W(CO)$_5$.[50]

Conclusions

The IR spectra of the rhodium(I), tungsten(0), and molybdenum(0) carbonyl complexes **2**, **4**, and **5** demonstrate clearly that the carbene–phosphinidene adducts **1a**–**1c** act as strong electron-donating phosphorus ligands; substantially lower CO stretching frequencies are observed in comparison with those of complexes with other important ancillary ligands such as phosphines and N-heterocyclic carbenes. In view of the potential application of carbene–phosphinidene ligands in homogeneous catalysis,[9] it can be concluded that these systems are particularly electron-rich additions to the large family of P-based ligands, whereas related cationic NHC-based phosphorus ligands such as phosphenium cations of the type [(NHC)PR$_2$]$^+$ were presented recently as electron-poor and strongly π-accepting ligands.[52] The NHC skeleton and also the phosphinidene moiety in NHC•PR ligands can be varied extensively to fine-tune the electronic and steric properties to adapt to the demands of a specific catalytic process.

Experimental Section

Materials and Instruments: All manipulations were performed under a strictly dry argon atmosphere by using standard Schlenk-line techniques and dry argon-filled gloveboxes. The solvents were dried with an MBraun solvent-purification system. The starting materials, carbene–phosphinidene adducts **1a**[15] and **1b**,[2] and the metal precursor [(Me$_3$N)W(CO)$_5$][39] were prepared according to previously published procedures. Dichloromesitylphosphine was prepared by a modified literature procedure (see Supporting Information for details). The ^{1}H, ^{13}C, and ^{31}P NMR spectra were recorded with Bruker DPX 200 (200 MHz) and Bruker AV 300 (300 MHz) spectrometers. The chemical shifts are given in ppm relative to residual solvent peaks {δ = 7.16 (C$_6$D$_6$), 3.58 ([D$_8$]THF) ppm}.[53] Coupling constants (*J*) are reported in Hz, and splitting patterns are indicated as s (singlet), d (doublet), t (triplet), m (multiplet), sept (septet), and br (broad). All spectra were recorded at room temperature. The IR spectra were recorded with a Bruker VERTEX 70 FTIR spectrometer equipped with a Pike Technologies MIRacle attenuated total reflectance (ATR) unit with neat samples unless otherwise noted. Elemental analyses were performed with a Vario Micro Cube system.

X-ray Structure Determinations: The crystallographic data are listed in Tables S1 and S2. Suitable single crystals were mounted on glass fibers in perfluorinated inert oil. The intensity measurements were performed at 100 K with an Oxford Diffraction Nova A diffractometer with mirror-focused Cu-K_α radiation. The diffractometer software CrysAlisPRO was employed.[54] Absorption corrections were based on multiscans. The structures were refined anisotropically on F^2 by using the SHELXL-97 program.[55] Hydrogen atoms were included by using a riding model or rigid methyl groups. Exceptions and special features: The PH hydrogen atoms H1 in **4a** and **5a** were found and refined freely. In these solvates, the THF molecules were refined as disordered over two positions with the less-occupied position isotropic. For **3**, residual electron density was interpreted as dichloromethane but was overlaid by other peaks that could not be interpreted. Therefore, the SQUEEZE program[56] was used to remove mathematically the effects of the solvent. For the calculations of the formula masses and associated parameters, idealized compositions were assumed. Compound **5a**·THF showed thermochromic behavior. At room temperature, the crystalline material was green-yellow, and it changed gradually to pink at –173 °C (see Figure S31 for pictures). The cell determination at room temperature gave approximately the same cell parameters as those determined at low temperature. The color change is reversible several times without the destruction of the single crystal.

CCDC 1440396 (for **1c**), 1440397 (for **4a**), 1440398 (for **4b**), 1440399 (for **4c**), 1440400 (for **5a**), 1440401 (for **5b**), and 1440402 (for **3**) contain the supplementary crystallographic data for this paper. These data can be obtained free of charge from The Cambridge Crystallographic Data Centre.

IPr·PMes (1c): $MesPCl_2$ (0.61 g, 2.74 mmol) was added slowly to a stirred suspension of IPr (1.066 g, 2.74 mmol) in *n*-hexane (150 mL). Immediately, a white precipitate formed. The mixture was then stirred at room temperature overnight. The white solid was collected by filtration, washed with *n*-hexane (3 × 20 mL), and dried under vacuum. Potassium graphite (0.742 g, 5.48 mmol) was added to the solid followed by THF (100 mL). The mixture was then stirred at room temperature overnight and filtered through a pad of Celite; all volatiles were removed under vacuum. The residue was washed with *n*-pentane and recrystallized from toluene at –78 °C to afford **1c** as a yellow solid, yield 0.118 g (8 % based on IPr). ^{1}H NMR ([D$_8$]THF, 300 MHz): δ = 7.46–6.72 (br m, 6 H, *m*-, *p*-$C_{Dipp}H$), 6.54 (s, 2 H, *m*-$C_{Mes}H$), 6.23 (s, 2 H, NC*H*), 3.28 (sept, $^3J_{H,H}$ = 6.8 Hz, 4 H, C*H*Me$_2$), 2.56 [s, 6 H, *o*-$C_{Mes}(CH_3)$], 2.06 [s, 3 H, *p*-$C_{Mes}(CH_3)$], 1.46 [br, 12 H, $CH(CH_3)_2$], 1.08 [br, 12 H, $CH(CH_3)_2$] ppm. ^{31}P{^{1}H} NMR ([D$_8$]THF, 121 MHz): δ = –51.3 (s) ppm. $C_{36}H_{47}N_2P$ (538.76): calcd. C 80.26, H 8.79, N 5.20; found C 80.50, H 8.79, N 5.16.

[(IPr·PPh){RhCl(CO)$_2$}] (2): [Rh(μ-Cl)(CO)$_2$]$_2$ (0.040 g, 0.102 mmol) in toluene (2 mL) was added slowly over 2 min to a stirred solution of **1b** (0.100 g, 0.201 mmol) in toluene (3 mL). After the addition of a few drops, the solution immediately became dark red, and a small amount of an orange precipitate formed. The mixture was stirred for 24 h and filtered. The solid was washed with *n*-hexane and dried under vacuum. The NMR spectroscopic data of this precipitate could not be recorded, but crystals were grown by slow evaporation of a CH_2Cl_2 solution at room temperature and shown to be the rhodium complex **3**. The solvent was removed from the filtrate, and the remaining solid was washed quickly with cold *n*-hexane (2 × 1 mL) and dried under vacuum to afford **2** as an orange solid, yield 0.087 g (62 % based on **1b**). ^{1}H NMR (C_6D_6, 300 MHz): δ = 7.93–7.87 (m, 2 H, *m*- or *o*-$C_{Ph}H$), 7.11–7.06 (m, 2 H, *p*-$C_{Dipp}H$), 6.96–6.95 (m, 4 H, *m*-$C_{Dipp}H$), 6.74–6.62 (m, 3 H, *m*- or *o*-$C_{Ph}H$ and *p*-$C_{Ph}H$), 6.44 (s, 2 H, NC*H*), 3.29 (sept, $^3J_{H,H}$ = 6.9 Hz, 4 H, C*H*Me$_2$), 1.53 [d, $^3J_{H,H}$ = 6.9 Hz, 12 H, $CH(CH_3)_2$], 0.93 [d, $^3J_{H,H}$ = 6.9 Hz, 12 H, $CH(CH_3)_2$] ppm. ^{13}C NMR (C_6D_6, 75 MHz): δ = 184.7 (dd, $^1J_{C,Rh}$ = 72.0, $^2J_{C,P}$ = 22.5 Hz, *cis* P–Rh–CO), 183.5 (dd, $^1J_{C,Rh}$ = 65.7, $^2J_{C,P}$ = 60.9 Hz, *trans* P–Rh–CO), 169.3 (d, $^1J_{C,P}$ = 98.2 Hz, C_{NHC}P), 146.4 (C_{Ar}), 139.0 (d, $^1J_{C,P}$ = 22.4 Hz, PC_{Ph}), 133.5 (C_{Ar}), 131.5 (C_{Ar}), 127.1 (d, $^3J_{C,P}$ = 9 Hz, C=*C*–N), 125.0 (C_{Ar}), 124.5 (d, $^3J_{P,C}$ = 3.7 Hz, *p*-C_{Ph}), 29.4 (d, $^5J_{C,P}$ = 3.3 Hz, *C*HMe$_2$), 26.6 [$CH(CH_3)_2$], 23.1 [d, $^6J_{C,P}$ = 1.8 Hz, $CH(CH_3)_2$] ppm. ^{31}P NMR (C_6D_6, 121 MHz): δ = –28.7 (d, $^1J_{P,Rh}$ = 48.4 Hz) ppm. $C_{35}H_{41}ClN_2O_2PRh$ (691.04): calcd. C 60.83, H 5.98, N 4.05; found C 61.19, H 6.22, N 4.08. IR: $\tilde{\nu}_{(CO)}$ = 2047 (s), 1965 (s) cm^{-1}.

[(IPr·PH)W(CO)$_5$]·THF (4a·THF): Compound **1a** (0.048 g, 0.115 mmol) and [(Me$_3$N)W(CO)$_5$] (0.044 g, 0.115 mmol) were dissolved in THF (10 mL). The reaction mixture was stirred for 16 h at 50 °C. All volatile components were removed under vacuum, and the residue was washed with *n*-hexane (3 mL). The remaining solid was dissolved in THF, and the solution was filtered through a pad of aluminum oxide. After the removal of the solvent under vacuum, **4a**·THF was isolated as a yellow solid, yield 0.054 g (57 % based on **1a**). ^{1}H NMR ([D$_8$]THF, 200 MHz): δ = 7.60–7.34 (m, 8 H, NC*H*, *p*-$C_{Dipp}H$, *m*-$C_{Dipp}H$), 2.79 (sept, $^3J_{H,H}$ = 6.7 Hz, 4 H, C*H*Me$_2$), 2.59 (d, $^1J_{H,P}$ = 215.2 Hz, 1 H, P*H*), 1.44 [d, $^3J_{H,H}$ = 6.7 Hz, 12 H, $CH(CH_3)_2$], 1.16 [d, $^3J_{H,H}$ = 6.8 Hz, 12 H, $CH(CH_3)_2$] ppm. ^{13}C{^{1}H} NMR ([D$_8$]THF, 50 MHz): δ = 199.8 (CO), 174.4 (C_{NHC}P), 146.3 (*o*-C_{Dipp}), 133.7 (NC_{Dipp}), 131.5 (*p*-C_{Dipp}), 125.5 (m-C_{Dipp}), 125.3 (d, $^3J_{C,P}$ = 3.2 Hz, C=*C*-N), 67.8 (THF), 29.3 (*C*HMe$_2$), 26.0 (THF), 25.3 [$CH(CH_3)_2$], 22.7 [$CH(CH_3)_2$] ppm. ^{31}P NMR ([D$_8$]THF, 81 MHz): δ = –163.4 (d, $^1J_{P,H}$ = 215.2, $^1J_{P,W}$ = 97.2 Hz) ppm. $C_{36}H_{45}N_2O_6PW$ (816.58): calcd. C 52.95, H 5.55, N 3.43; found C 53.52, H 5.64, N 3.63. IR: $\tilde{\nu}_{(CO)}$ = 2055 (m), 1961 (w), 1902 (s), 1861 (s) cm^{-1}.

[(IPr·PPh)W(CO)$_5$] (4b). Procedure A: Carbene–phosphinidene adduct **1b** (0.100 g, 0.201 mmol) and [(Me$_3$N)W(CO)$_5$] (0.077 g, 0.201 mmol) were dissolved in THF (20 mL) at room temperature. The reaction mixture was stirred for 16 h at 50 °C. All volatile components were removed under vacuum, and unreacted [(Me$_3$N)W(CO)$_5$] was extracted with *n*-hexane (5 mL). The remaining solid was then dissolved in THF, and the solution was filtered through a pad of aluminum oxide. The solvent was removed under vacuum to give the air-stable complex **4b** as a yellow solid, yield 0.095 g (58 % based on **1b**).

Procedure B: W(CO)$_6$ (0.352 g, 1.000 mmol) was suspended in THF (60 mL), and the suspension was degassed with three freeze–pump–thaw cycles. The suspension was irradiated with UV light for 4 h. To this solution, **1b** (0.497 g, 1.000 mmol) dissolved in THF (10 mL) was added. The reaction mixture was stirred at room temperature overnight. The solution was concentrated to 10 mL and stored at –35 °C for 5 d to afford **4b** as a crystalline solid. Further concentration and cooling of the mother liquor yielded small amounts of **4b**, yield 0.279 g (34 % based on **1b**). ^{1}H NMR ([D$_8$]THF, 300 MHz): δ = 7.50 (s, 2 H, NC*H*), 7.44 (t, $^3J_{H,H}$ = 7.7 Hz, 2 H, *p*-$C_{Dipp}H$), 7.27 (d, $^3J_{H,H}$ = 7.7 Hz, 4 H, *m*-$C_{Dipp}H$), 7.13–7.06 (m, 2 H, *m*-$C_{Ph}H$), 6.88–6.81 (m, 1 H, *p*-$C_{Ph}H$), 6.75–6.68 (m, 2 H, *o*-$C_{Ph}H$), 2.95 (sept, $^3J_{H,H}$ = 6.8 Hz, 4 H, C*H*Me$_2$), 1.35 [d, $^3J_{H,H}$ = 6.8 Hz, 12 H, $CH(CH_3)_2$], 1.12 [d, $^3J_{H,H}$ = 6.8 Hz, 12 H, $CH(CH_3)_2$] ppm. ^{13}C{^{1}H} NMR ([D$_8$]THF, 75 MHz): δ = 200.9 (CO), 146.3 (*o*-C_{Dipp}), 138.9 (d, $^1J_{P,C}$ = 22.5 Hz, PC_{Ph}), 135.2 (NC_{Dipp}), 131.6 (*p*-C_{Dipp}), 127.7 (*p*-C_{Ph}), 127.2 (d,

$^{2}J_{\mathrm{P,C}}$ = 8.7 Hz, *o*-C_{Ph}), 126.7 (d, $^{2}J_{\mathrm{C,P}}$ = 3.0 Hz, *m*-C_{Ph}), 125.5 (*m*-C_{Dipp}), 125.4 (d, $^{3}J_{\mathrm{C,P}}$ = 5.0 Hz, C=*C*-N), 29.9 (*C*HMe$_2$), 26.0 [CH(*C*H$_3$)$_2$], 22.7 [CH(*C*H$_3$)$_2$] ppm. ^{31}P{^{1}H} NMR ([D$_8$]THF, 121 MHz): δ = 57.7 (s, $^{1}J_{\mathrm{P,W}}$ = 120.5 Hz) ppm. $C_{38}H_{41}N_2O_5PW$ (820.57): calcd. C 55.62, H 5.04, N 3.41; found C 55.89, H 4.83, N 2.97. IR: $\tilde{\nu}_{(\mathrm{CO})}$ = 2054 (m), 1963 (w), 1909 (s), 1860 (s) cm^{-1}.

[(IPr·PMes)W(CO)$_5$] (4c): Carbene–phosphinidene adduct **1c** (0.054 g, 0.100 mmol) and [(Me$_3$N)W(CO)$_5$] (0.038 g, 0.100 mmol) were dissolved in THF (10 mL). The reaction mixture was stirred for 16 h at 50 °C. All volatile components were removed under vacuum, and the residue was washed with *n*-hexane (3 mL). The remaining solid was dissolved in THF, and the solution was filtered through a pad of aluminum oxide. The removal of the solvent gave **4c** as a yellow solid, yield 0.016 g (18 % based on **1c**). ^{1}H NMR ([D$_8$]THF, 200 MHz): δ = 7.54–7.22 (br m, 8 H, NC*H*, *m*, *p*-C_{Dipp}*H*), 6.59 (s, 2 H, *m*-C_{Mes}*H*), 2.76 (sept, $^{3}J_{\mathrm{H,H}}$ = 6.8 Hz, 4 H, C*H*Me$_2$), 2.25 [s, 6 H, *o*-C_{Mes}(C*H*$_3$)], 2.10 [s, 3 H, *p*-C_{Mes}(C*H*$_3$)], 1.34 [d, $^{3}J_{\mathrm{H,H}}$ = 6.8 Hz, 12 H, CH(C*H*$_3$)$_2$], 1.09 [d, $^{3}J_{\mathrm{H,H}}$ = 6.8 Hz, 12 H, CH(C*H*$_3$)$_2$] ppm. ^{13}C{^{1}H} NMR ([D$_8$]THF, 75 MHz): δ = 201.6 (*C*O), 149.5 (*o*-C_{Dipp}), 145.5 (d, $^{1}J_{\mathrm{C,P}}$ = 12.8 Hz, PC_{Mes}), 142.9 (NC_{Dipp}), 139.5 (*p*-C_{Mes}), 138.2 (*o*-C_{Mes}), 134.0 (*m*-C_{Mes}), 132.1 (d, $^{3}J_{\mathrm{C,P}}$ = 5.3 Hz, C=*C*–N), 128.8 (*p*-C_{Dipp}), 128.5 (*m*-C_{Dipp}), 127.9 (*p*-C_{Dipp}), 32.5 (*o*-$CH_{3,\mathrm{Mes}}$), 29.1 (*C*HMe$_2$), 28.6 [CH(*C*H$_3$)$_2$], 25.4 [CH(*C*H$_3$)$_2$], 23.6 (*p*-$CH_{3,\mathrm{Mes}}$) ppm. ^{31}P{^{1}H} NMR ([D$_8$]THF, 81 MHz): δ = –95.1 (s, $^{1}J_{\mathrm{P,W}}$ = 159.5 Hz) ppm. $C_{41}H_{47}N_2O_5PW$ (862.65): calcd. C 57.09, H 5.49, N 3.25; found C 55.74, H 5.75, N 3.65. IR: $\tilde{\nu}_{(\mathrm{CO})}$ = 2058 (m), 1963 (w), 1911 (s), 1870 (s) cm^{-1}.

[(IPr·PH)Mo(CO)$_5$]·THF (5a·THF): Mo(CO)$_6$ (0.055 g, 0.208 mmol) was suspended in THF (20 mL), and the suspension was degassed with three freeze–pump–thaw cycles. The suspension was heated under reflux for 6 h. After the addition of **1a** (0.087 g, 0.208 mmol) in THF (10 mL) to the hot solution, the mixture was stirred at room temperature overnight. All volatiles were then removed under vacuum. The remaining solid was dissolved in THF, and the solution was filtered through a pad of aluminum oxide. The solvent was removed to afford **5a**·THF as a pale green solid, yield 0.102 g (67 % based on **1a**). ^{1}H NMR ([D$_8$]THF, 200 MHz): δ = 7.59–7.35 (m, 8 H, NC*H*, *p*-C_{Dipp}*H*, *m*-C_{Dipp}*H*), 2.80 (sept, $^{3}J_{\mathrm{H,H}}$ = 6.8 Hz, 4 H, C*H*Me$_2$), 2.18 (d, $^{1}J_{\mathrm{H,P}}$ = 211.6 Hz, 1 H, P*H*), 1.44 [d, $^{3}J_{\mathrm{H,H}}$ = 6.8 Hz, 12 H, CH(C*H*$_3$)$_2$], 1.16 [d, $^{3}J_{\mathrm{H,H}}$ = 6.8 Hz, 12 H, CH(C*H*$_3$)$_2$] ppm. ^{13}C{^{1}H} NMR ([D$_8$]THF, 75 MHz): δ = 208.7 (*C*O), 176.2 (d, $^{1}J_{\mathrm{C,P}}$ = 83.1 Hz, C_{NHC}P), 146.7 (*o*-C_{Dipp}), 134.2 (NC_{Dipp}), 131.8 (*p*-C_{Dipp}), 125.8 (m-C_{Dipp}), 125.4 (d, $^{3}J_{\mathrm{P,C}}$ = 2.9 Hz, C=*C*–N), 68.2 (coordinated THF), 29.7 (*C*HMe$_2$), 26.4 (coordinated THF), 25.7 [CH(*C*H$_3$)$_2$], 23.2 [CH(*C*H$_3$)$_2$] ppm. ^{31}P NMR ([D$_8$]THF, 81 MHz): δ = 147.1 (d, $^{1}J_{\mathrm{P,H}}$ = 211.6 Hz) ppm. $C_{36}H_{45}N_2O_6PMo$ (728.70): calcd. C 59.34, H 6.22, N 3.84; found C 60.37, H 6.35, N 4.03. IR: $\tilde{\nu}_{(\mathrm{CO})}$ = 2057 (m), 1970 (w), 1910 (s), 1866 (s) cm^{-1}.

[(IPr·PPh)Mo(CO)$_5$] (5b): Mo(CO)$_6$ (0.055 g, 0.210 mmol) was suspended in THF (25 mL), and the suspension was degassed with three freeze–pump–thaw cycles. The suspension was heated under reflux for 8 h. To this hot solution, **1b** (0.104 g, 0.210 mmol) in THF (10 mL) was added, and the mixture was stirred at room temperature for 16 h. All volatile components were removed under vacuum. The remaining solid was dissolved in THF, and the solution was filtered through a pad of aluminum oxide. The removal of the solvent gave the air-stable complex **5b** as a yellow solid, yield 0.092 g (60 % based on **1b**). ^{1}H NMR ([D$_8$]THF, 200 MHz): δ = 7.45 (s, 2 H, NC*H*), 7.43 (*t*, $^{3}J_{\mathrm{H,H}}$ = 7.7 Hz, 2 H, *p*-C_{Dipp}*H*), 7.26 (d, $^{3}J_{\mathrm{H,H}}$ = 7.7 Hz, 4 H, *m*-C_{Dipp}*H*), 7.17–7.05 (m, 2 H, *m*-C_{Ph}*H*), 6.88–6.79 (m, 1 H, *p*-C_{Ph}*H*), 6.75–6.64 (m, 2 H, *o*-C_{Ph}*H*), 2.97 (sept, $^{3}J_{\mathrm{H,H}}$ = 6.7 Hz, 4 H, C*H*Me$_2$), 1.36 [d, $^{3}J_{\mathrm{H,H}}$ = 6.7 Hz, 12 H, CH(C*H*$_3$)$_2$], 1.12 [d, $^{3}J_{\mathrm{H,H}}$ = 6.7 Hz, 12 H, CH(C*H*$_3$)$_2$] ppm. A ^{13}C NMR spectrum could not be recorded because of the low solubility of **5b**. ^{31}P{^{1}H} NMR ([D$_8$]THF, 81 MHz): δ = –40.2 (s) ppm. $C_{38}H_{41}N_2O_5PMo$ (732.69): calcd. C 62.29, H 5.64, N 3.82; found C 62.22, H 5.69, N 3.77. IR: $\tilde{\nu}_{(\mathrm{CO})}$ = 2055 (m), 1970 (w), 1915 (s), 1864 (s) cm^{-1}.

Acknowledgments

This work was supported by the Deutsche Forschungsgemeinschaft (DFG) through grant TA 189/16-1.

Keywords: P ligands · Carbonyl ligands · Rhodium · Tungsten · IR spectroscopy

[1] a) A. J. Arduengo, H. V. Rasika Dias, J. C. Calabrese, *Chem. Lett.* **1997**, 143–144; b) A. J. Arduengo III, J. C. Calabrese, A. H. Cowley, H. V. R. Dias, J. R. Goerlich, W. J. Marshall, B. Riegel, *Inorg. Chem.* **1997**, *36*, 2151–2158.

[2] O. Back, M. Henry-Ellinger, C. D. Martin, D. Martin, G. Bertrand, *Angew. Chem. Int. Ed.* **2013**, *52*, 2939–2943; *Angew. Chem.* **2013**, *125*, 3011.

[3] a) D. Himmel, I. Krossing, A. Schnepf, *Angew. Chem. Int. Ed.* **2014**, *53*, 370–374; *Angew. Chem.* **2014**, *126*, 378; b) G. Frenking, *Angew. Chem. Int. Ed.* **2014**, *53*, 6040–6046; *Angew. Chem.* **2014**, *126*, 6152; c) D. Himmel, I. Krossing, A. Schnepf, *Angew. Chem. Int. Ed.* **2014**, *53*, 6047–6048; *Angew. Chem.* **2014**, *126*, 6159.

[4] a) P. Rosa, C. Gouverd, G. Bernardinelli, T. Berclaz, M. Geoffroy, *J. Phys. Chem. A* **2003**, *107*, 4883–4892; b) G. Frison, A. Sevin, *J. Organomet. Chem.* **2002**, *643–644*, 105–111.

[5] L. Weber, *Eur. J. Inorg. Chem.* **2000**, 2425–2441.

[6] A. J. Arduengo III, C. J. Carmalt, J. A. C. Clyburne, A. H. Cowley, R. Pyati, *Chem. Commun.* **1997**, 981–982.

[7] a) K. Schwedtmann, M. H. Holthausen, K.-O. Feldmann, J. J. Weigand, *Angew. Chem. Int. Ed.* **2013**, *52*, 14204; *Angew. Chem.* **2013**, *125*, 14454–14458; b) M. Alcarazo, K. Radkowski, G. Mehler, R. Goddard, A. Fürstner, *Chem. Commun.* **2013**, *49*, 3140.

[8] V. A. K. Adiraju, M. Yousufuddin, H. V. R. Dias, *Dalton Trans.* **2015**, *44*, 4449–4454.

[9] A. Doddi, D. Bockfeld, P. G. Jones, M. Tamm, *Chem. Eur. J.* **2015**, *21*, 16178–16189.

[10] T. G. Larocque, G. G. Lavoie, *New J. Chem.* **2014**, *38*, 499–502.

[11] a) K. Hansen, T. Szilvási, B. Blom, E. Irran, M. Driess, *Chem. Eur. J.* **2014**, *20*, 1947–1956; b) K. Hansen, T. Szilvási, B. Blom, S. Inoue, J. Epping, M. Driess, *J. Am. Chem. Soc.* **2013**, *135*, 11795–11798.

[12] A. M. Tondreau, Z. Benkö, J. R. Harmer, H. Grützmacher, *Chem. Sci.* **2014**, *5*, 1545–1554.

[13] M. Cicač-Hudi, J. Bender, S. H. Schlindwein, M. Bispinghoff, M. Nieger, H. Grützmacher, D. Gudat, *Eur. J. Inorg. Chem.* **2016**, 649–658.

[14] L. Liu, D. A. Ruiz, F. Dahcheh, G. Bertrand, *Chem. Commun.* **2015**, *51*, 12732–12735.

[15] A. Doddi, D. Bockfeld, T. Bannenberg, P. G. Jones, M. Tamm, *Angew. Chem. Int. Ed.* **2014**, *53*, 13568–13572; *Angew. Chem.* **2014**, *126*, 13786.

[16] a) L. Weber, S. Kleinebekel, A. Rühlicke, H.-G. Stammler, B. Neumann, *Eur. J. Inorg. Chem.* **2000**, 1185–1191; b) L. Weber, O. Kaminski, H.-G. Stammler, B. Neumann, V. D. Romanenko, *Z. Naturforsch. B* **1993**, *48*, 1784–1794.

[17] M. Bispinghoff, A. M. Tondreau, H. Grützmacher, C. A. Faradji, P. G. Pringle, *Dalton Trans.* **2016**, *45*, 5999–6003.

[18] A. Fürstner, M. Alcarazo, H. Krause, C. W. Lehmann, *J. Am. Chem. Soc.* **2007**, *129*, 12676–12677.

[19] A. R. Chianese, X. Li, M. C. Janzen, J. W. Faller, R. H. Crabtree, *Organometallics* **2003**, *22*, 1663–1667.

[20] T. Dröge, F. Glorius, *Angew. Chem. Int. Ed.* **2010**, *49*, 6940–6952; *Angew. Chem.* **2010**, *122*, 7094.

[21] J. Huheey, E. Keiter, R. Keiter, *Anorganische Chemie: Prinzipien von Struktur und Reaktivität*, de Gruyter, Berlin, **1995**.

[22] a) F. Mathey, Z. Duan, *Dalton Trans.* **2016**, *45*, 1804–1809; b) F. Mathey, *Dalton Trans.* **2007**, 1861; c) F. Mathey, *Angew. Chem. Int. Ed.* **2003**, *42*, 1578–1604; *Angew. Chem.* **2003**, *115*, 1616; d) F. Mathey, Huy, H. T. Ngoc, A. Marinetti, *Helv. Chim. Acta* **2001**, *84*, 2938–2957; e) F. Mathey, *Angew. Chem. Int. Ed. Engl.* **1987**, *26*, 275–286; *Angew. Chem.* **1987**, *99*, 285.

[23] N. H. Tran Huy, B. Donnadieu, G. Bertrand, F. Mathey, *Chem. Asian J.* **2009**, *4*, 1225–1228.

[24] M. Klein, G. Schnakenburg, A. Espinosa Ferao, N. Tokitoh, R. Streubel, *Eur. J. Inorg. Chem.* **2016**, 685–690.

[25] a) E. Rotondo, G. Battaglia, G. Giordano, F. P. Cusmano, *J. Organomet. Chem.* **1993**, 245–252; b) W. A. Herrmann, J. Schütz, G. D. Frey, E. Herdtweck, *Organometallics* **2006**, *25*, 2437–2448.

[26] C. A. Tolman, *Chem. Rev.* **1977**, *77*, 313–348.

[27] A. Fürstner, M. Alcarazo, R. Goddard, C. W. Lehmann, *Angew. Chem. Int. Ed.* **2008**, *47*, 3210–3214; *Angew. Chem.* **2008**, *120*, 3254.

[28] C. A. Tolman, *J. Am. Chem. Soc.* **1970**, *92*, 2953–2956.

[29] T. Sato, Y. Hirose, D. Yoshioka, S. Oi, *Organometallics* **2012**, *31*, 6995–7003.

[30] C. A. Urbina-Blanco, X. Bantreil, H. Clavier, A. M. Z. Slawin, S. P. Nolan, *Beilstein J. Org. Chem.* **2010**, *6*, 1120–1126.

[31] C. A. Dyker, V. Lavallo, B. Donnadieu, G. Bertrand, *Angew. Chem. Int. Ed.* **2008**, *47*, 3206–3209; *Angew. Chem.* **2008**, *120*, 3250.

[32] K. Powers, C. Hering-Junghans, R. McDonald, M. J. Ferguson, E. Rivard, *Polyhedron* **2016**, 8–14.

[33] S. Kronig, P. G. Jones, M. Tamm, *Eur. J. Inorg. Chem.* **2013**, 2301–2314.

[34] K. Fourmy, S. Mallet-Ladeira, O. Dechy-Cabaret, M. Gouygou, *Organometallics* **2013**, *32*, 1571–1574.

[35] G. Canepa, C. D. Brandt, H. Werner, *Organometallics* **2004**, *23*, 1140–1152.

[36] S. Wolf, H. Plenio, *J. Organomet. Chem.* **2009**, *694*, 1487–1492.

[37] A. Winkler, M. Freytag, P. G. Jones, M. Tamm, *J. Organomet. Chem.* **2015**, *775*, 164–168.

[38] K. Pal, O. B. Hemming, B. M. Day, T. Pugh, D. J. Evans, R. A. Layfield, *Angew. Chem. Int. Ed.* **2016**, *55*, 1690–1693; *Angew. Chem.* **2016**, *128*, 1722–1725.

[39] W. Strohmeier, J. F. Guttenberger, H. Blumenthal, G. Albert, *Chem. Ber.* **1966**, *99*, 3419–3424.

[40] H. Werner, R. Prinz, *J. Organomet. Chem.* **1966**, *5*, 79–89.

[41] L. Weber, M. Meyer, H.-G. Stammler, B. Neumann, *Chem. Eur. J.* **2001**, *7*, 5401–5408.

[42] T. J. Malosh, S. R. Wilson, J. R. Shapley, *Inorg. Chim. Acta* **2009**, *362*, 2849–2855.

[43] M. J. Aroney, I. E. Buys, M. S. Davies, T. W. Hambley, *J. Chem. Soc., Dalton Trans.* **1994**, 2827–2834.

[44] F. A. Cotton, D. J. Darensbourg, W. H. Ilsley, *Inorg. Chem.* **1981**, *20*, 578–583.

[45] C. Murcia-García, A. Bauzá, G. Schnakenburg, A. Frontera, R. Streubel, *CrystEngComm* **2015**, *17*, 1769–1772.

[46] a) F. A. Cotton, C. S. Kraihanzel, *J. Am. Chem. Soc.* **1962**, *84*, 4432–4438; b) L. E. Orgel, *Inorg. Chem.* **1962**, *1*, 25–29.

[47] R. L. Keiter, J. G. Verkade, *Inorg. Chem.* **1969**, *8*, 2115–2120.

[48] G. M. Bancroft, L. Dignard-Bailey, R. J. Puddephatt, *Inorg. Chem.* **1986**, *25*, 3675–3680.

[49] H. Schumann, L. Rösch, H.-J. Kroth, J. Pickardt, H. Neumann, B. Neudert, *Z. Anorg. Allg. Chem.* **1977**, *430*, 51–60.

[50] S. M. I. Al-Rafia, A. C. Malcolm, S. K. Liew, M. J. Ferguson, E. Rivard, *J. Am. Chem. Soc.* **2011**, *133*, 777–779.

[51] M. Ardon, G. Hogarth, D. T. Oscroft, *J. Organomet. Chem.* **2004**, *689*, 2429–2435.

[52] a) J. Carreras, G. Gopakumar, L. Gu, A. Gimeno, P. Linowski, J. Petuškova, W. Thiel, M. Alcarazo, *J. Am. Chem. Soc.* **2013**, *135*, 18815–18823; b) M. Alcarazo, *Chem. Eur. J.* **2014**, *20*, 7868–7877.

[53] G. R. Fulmer, A. J. M. Miller, N. H. Sherden, H. E. Gottlieb, A. Nudelman, B. M. Stoltz, J. E. Bercaw, K. I. Goldberg, *Organometallics* **2010**, *29*, 2176–2179.

[54] *CrysAlisPRO*, Oxford Diffraction/Agilent Technologies UK Ltd., Yarnton, UK.

[55] G. M. Sheldrick, *Acta Crystallogr., Sect. A* **2008**, *64*, 112–122.

[56] *SQUEEZE (part of the PLATON program suite)*, A. L. Spek, University of Utrecht, The Netherlands, **2015**.

Received: April 26, 2016